Appendix 1

Volcanic system summaries

This appendix provides a summary of the published information for each of the studied volcanoes, organized by arc. First, we review the eruptive activity, composition of magmas, and evidence for water content reported here. Except where noted, general information (e.g., elevation, eruptive history, common rock types) is from the Smithsonian Global Volcanism Program. References for magmatic water content are given individually. Second, we review studies of magma storage. All depths are given with reference to the surface elevation (the summit elevation in many cases), and where the original publication gave the depth with a difference reference (e.g., reference to sea level), we also give the original depth in parentheses. Several assumptions are made in the compilation:

- If the reference frame used in the original publication is not clear, the depth is assumed to be referenced to the surface elevation.
- If the lateral location of the storage region is not specified, it is assumed storage occurs directly below the summit.
- If the magma reservoir is shown to be off axis, the depth is reported relative to the surface elevation (obtained using Google Earth) above the proposed region of storage.

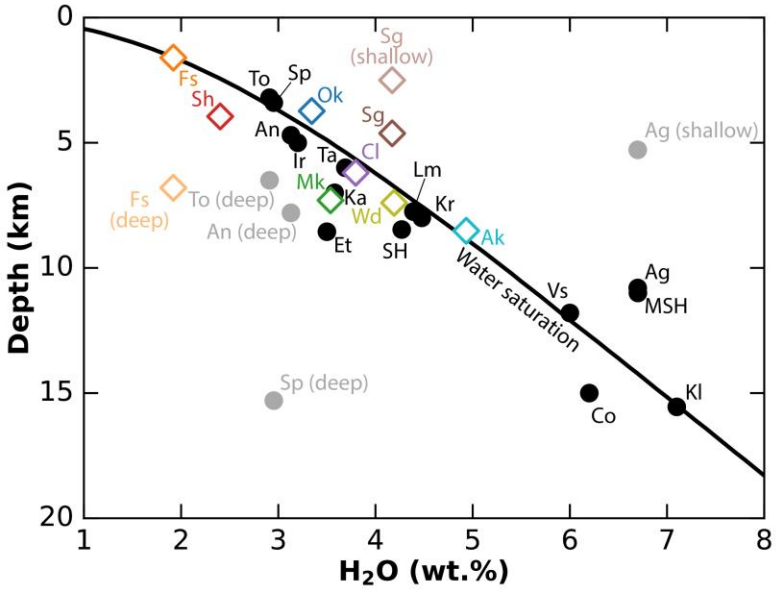

Figure 1. Labeled geophysical estimates of magma storage depth and magmatic water content (n = 24). The water saturation line is plotted (modeled for basalt with 49 wt.% SiO_2 at a temperature of 1100 °C using Newman and Lowenstern, 2002). Some volcanoes have multiple storage regions that have been identified, which are shown with both dark and light samples, indicating that magma storage at water saturation is an important, but not the only, depth of magma storage. Volcanoes include Ag – Augustine, Ak – Akutan, An – Anatahan, Cl – Cleveland, Co – Colima, Et – Etna, Fs – Fisher, Ir – Irazú, Ka – Karymsky, Kl – Kliuchevskoy, Kr – Korovin, Lm – Llaima, Mk –

Makushin, MSH – Mount St. Helens, Ok – Okmok, SH – Soufrière Hills, Sh – Shishaldin, Sg – Seguam, Sp – Spurr, Ta – Tanaga, To – Tolbachik, Vs – Vesuvius, Wd – Westdahl.

Alaska-Aleutian arc

Akutan (Ak)

Akutan volcano (1303 m), located in the Central Aleutian arc, is a stratovolcano with a 2 km caldera at the summit. Most of the eruptions at Akutan are basalt to andesite in composition. Akutan has been highly active over the last century, having 24 reported eruptions (23 confirmed) with the most recent having occurred in 1992. Most eruptions have had a volcanic explosivity index (VEI) of 2. Zimmer et al. (2010) reported 39 olivine-, clinopyroxene-, and plagioclase-hosted melt inclusions compositions, and Rasmussen et al. (*in prep*) reported 14 olivine-hosted melt inclusion compositions. Melt compositions are mostly basalt to andesite, with rare dacite to rhyolite composition in clinopyroxene- and plagioclase-hosted melt inclusions. Water contents are variable. The maximum water content (4.9 wt.%) was reported by Rasmussen et al. (*in prep*), which is from a sample collected at the summit (AK16TAP96) that is believed to be produced in an historical eruption.

Several seismic and geodetic studies have investigated magma storage below Akutan volcano. We focus our attention on the three most recent studies. Janiszewski et al. (2013) investigated receiver functions along the length of the Aleutians. They noted a strong arrival at each of their three stations, consistent with a large magma body, at depths of 7-10 km, 8.5-10.5 km, and 8-9 km. Lu and Dzurisin (2014) reviewed 20 years of InSAR data at Akutan volcano. During 1992-2002, surface uplift of about 1.0 cm/year was detected. The deformation patterns are consistent with point source (Mogi, 1958) inflation at 6.3-8.3 km depth (5-7 km BSL), which was interpreted to be a region of long-term storage. In 1996, 2 days of intense seismicity occurred at depths of 1.3-9.3 km (0-8 km BSL), which was interpreted to be the result of a dike that did not reach the surface. Inflation during 2004-2009 was also detected, which was similar to patterns seen in the 1992-2002 deformation. Finally, Syracuse et al. (2015) applied joint body and surface wave tomography to Akutan. They suggested a long-term region of magma storage is located at 8.3-11.3 km depth (7-10 km BSL). The authors noted that their depths are slightly greater than those suggested by Lu and Dzurisin (2014), and they suggested that deformation may occur near the top of their proposed storage region which overlaps with the high end of the depth range given by Lu and Dzurisin (2014). We consider depths reported by all 3 studies, which are relatively consistent.

Augustine (Ag)

Augustine volcano is an active volcano in the eastern Aleutian arc. The edifice, rising 1252 m above sea level, is composed of a central dome built by repeated episodes of dome growth. The composition of typical erupted products ranges from basaltic-andesite to dacite. There have been 6 confirmed eruptions in the last century, spanning VEI 1 to 4. The most recent eruption occurred in 2005. Zimmer et al. (2010) measured the composition of 57 olivine-hosted melt inclusions from Augustine. They reported a maximum water content of 6.7 wt.%, which is in a melt inclusion from a basaltic hyaloclastite (05AUNY-10).

Lu and Dzurisin (2014) evaluated InSAR and GPS data collected at Augustine between 1992-2005, which includes the run-up to the 2006 eruption. Deformation during this period was attributed to a contracting point source at 3.3-5.3 km depth (2-4 km BSL) and an inflating point source at 8.3-13.3 km depth (7-12 km BSL). The latter was suggested to be a zone of long-term magma storage. The shallower source may be another region of magma storage, and the observed contraction could be a result of cooling and degassing. The authors also evaluated post-eruptive subsidence that occurred from 2006-2010. However, much of the deformation signal produced during this period was attributed to subsidence of pyroclastic and lava flows produced in 1986 and 2006, and volcano-wide deformation patterns are less apparent. We consider both reservoirs but note that the deeper reservoir (8.3-13.3 km) may be a longer-lived reservoir.

Cleveland (Cl)

Cleveland volcano (1730 m) is a highly active, symmetrical stratovolcano. Limited work has been conducted on Cleveland owing to its remote location in the Central Aleutians. Nicolaysen and Izbekov (unpublished) have collected historical lavas, and most are basaltic-andesite to andesite in composition. Over the last 30 years, there have been 15 reported (13 confirmed) eruptions, indicating Cleveland is one of the most active volcanoes in the Aleutian arc. In Chapter 3 of this dissertation the compositions of 39 olivine-, clinopyroxene-, and plagioclase-hosted melt inclusions, of which 26 are attributed to summit eruptions, were reported. The maximum observed water content in the summit samples is 3.8 wt.%, which is in an ash sample (CV15DJR09E) collected from a stream cut on the south flank.

Insight into the plumbing system at Cleveland volcano comes from the multidisciplinary study of Power et al. (*in prep*). The authors report on a seismic survey was conducted between 2015-2016. A locust of earthquakes was found between depths of 4.7-7.7 km (3-6 km BSL), which is suggested to be a region of magma accumulation.

Fisher (Fs)

Fisher caldera (1112 m) is a large caldera (11 x 18 km) in the Central Aleutian arc. The caldera is the remnant of an andesitic stratovolcano that experienced a caldera forming eruption at 9.4 ka (Stelling et al., 2005). The edifice is comprised mostly of basaltic to andesitic rocks. The most recent eruption may have occurred in 1830, although this event is unconfirmed (AVO). Fisher caldera has been geodetically active within the last 30 years (Lu and Dzurisin, 2014), which may indicate the system is magmatically active. In Chapter 5 of this dissertation, we report 27 melt inclusion compositions from Fisher, of which 3 belong to a sample from Mt. Finch (Cone3-2A) that is related to the main volcanic system (i.e., not flank or side cone eruptions). These melt inclusions are basalt to basaltic-andesite in composition. The maximum water content recorded is 1.9 wt.%.

Two geodetic studies have investigated magma storage below Fisher caldera. Mann et al. (2002) used GPS data to investigate deformation occurring at Fisher caldera between 1998 and 2001. During this time, Fisher underwent subsidence. There had been no recent eruption. The authors attributed the ground motion to cooling and crystallization of a shallow magma body or the release of pressure in a shallow hydrothermal system. They suggested both potential causes are linked to

magma intrusion. Assuming a Mogi (1958) source, they determined the deformation is localized to $1.6^{+2.6}_{-1.4}$ km below the surface. Lu and Dzurisin (2014) investigated InSAR data collected from 2003-2010. They observed minor (1.5 cm/year) subsidence over this period. They modeled the source of the subsidence as a point (Mogi, 1958), sill (Okada, 1985), and a spheroid (Yang et al., 1988). The source depth for each of the models they test are 4.6-7.5 km, 6.6-9.6 km, and 4.6-6.6 km, respectively. The authors did not give preference to one model because the geodetic signal is minor and there is uncertainty in the depth of the source. Given the uncertainty of the source of the InSAR detected deformation (e.g., sill or point source), we prefer the model given by Mann and Freymuller (2003) and report a depth of 1.6 km. We also have displayed the greater depths from Lu and Dzurisin (2014) as a separate region of magma storage.

Korovin (Kr)

Korovin volcano (1518 m) is a stratocone in the Atka volcanic complex of the Western Aleutian arc. The cone is built primarily of basalts, but andesites and dacites also occur. Over the last 20 years, there have been 5 confirmed eruptions (4 VEI 1 eruptions and 1 VEI 3 eruption); the most recent of which occurred in 2006. Zimmer et al. (2010) presented data from 13 olivine-hosted and 2 plagioclase-hosted melt inclusions. The maximum water content measured (4.5 wt.%) is in an olivine-hosted melt inclusion from sample KTS404T5, a basaltic andesite collected from a tephra section.

InSAR images collected during 1997-2007 were studied by Lu and Dzurisin (2014). During this time span the broad deformational trend was inflation, with occasional periods of deflation or little-no geodetic activity. Inflation rate increased rapidly in 1996-1997, coincident with a seismic swarm. Both initiated before a small eruption in late 1996. Deformation was modeled as a Mogi (1958) source. The results indicated magma accumulation in a reservoir located at 6.4-9.4 km depth (5-8 km BSL) below Kliuchef volcano (1416 m), which is ~6 km south of Korovin. Contraction prior to 2006 was centered below Korovin at a depth of 4.5-5.5 km (3-4 km BSL), which was attributed to cooling and degassing from the upper part of the magmatic or hydrothermal systems. The authors suggested the deeper source (6.4-9.4 km) is the likely region of magma storage for Korovin, and we use this depth range for our work.

Makushin (Mk)

Located in the Central Aleutian arc, Makushin volcano (1800 m) is a stratovolcano with a 2.5 km diameter caldera at the summit. Pakushin, a composite cone, is a prominent feature on the SW flank. Most of the edifice is basalt to andesite in composition. There has been 9 reported (7 confirmed) eruptions in the last century, mostly VEI 1 or 2. Zimmer et al. (2010) presented 26 olivine- and pyroxene-hosted melt inclusion data from Pakushin and Angela's Cone (another cone on Makushin). In Chapter 5 of this dissertation we report on 15 olivine-hosted melt inclusions from Pakushin and Tabletop (a cinder cone on the lower flank of Makushin). The maximum water of 3.5 wt.% is recorded in a clinopyroxene-hosted melt inclusion, which is from a tephra sample (05EKPK-54B) collected near the base of Pakushin containing lapilli and bombs.

Two recent studies investigated the magmatic plumbing system below Makushin. Lu and Dzurisin (2014) evaluated InSAR images collected during 1993-2000 and 2004-2009. They noted that a

total of 7 cm of surface uplift occurred from 1993-1995, and from 1995-2000, minor subsidence occurred. Subsidence continued during 2004-2009 at about the same rate (~1 cm/year) as during 1995-2000. They suggested the 1993-1995 inflation was due to magma accumulation before the 1995 eruption, which they modeled as a point source 5 km east of the summit (~800 m elevation) at ~7.8 km depth (7 km BSL). The authors modeled subsidence during the 2004-2009 period as point (Mogi, 1958) and sill (Okada, 1985) sources, obtaining depth estimates of 6.6 km (5.8 km BSL) and 7.2 km (6.4 km BSL), respectively. The authors noted that Bridges and Gao (2006) conducted a survey of seismic data collected between 2001-2005 in which they found high seismic b-values in the 4.8-7.8 km depth (4-7 km BSL) region, which was suggested to be a region with a high crack density above a magma reservoir. Taking the observations together, Lu and Dzurisin (2014) proposed a magma storage region at 5.8-7.8 km (5-7 km BSL). Syracuse et al. (2015) conducted surface and body wave tomography to evaluate the magmatic plumbing system below Makushin volcano. They noted that above 5.8 km depth (5 km BSL), the velocity structure is complex. In general, high P-wave velocity regions are located under the caldera and cones. Below 5.8 km depth (5 km BSL), velocities decrease reaching a minimum at 9.3 km (7.5 km BSL). The authors suggested that a magma reservoir is located at about 8.8 km depth (6.8-11.8 km deep, or 5-10 km BSL, based on their Fig. 7). We consider both depth estimates (5.8-7.8 km and 6.8-11.8 km).

Okmok (Ok)

Okmok is a large shield volcano in the Central Aleutian arc with 2 superimposed calderas (~500 m elevation at floor) that formed at 12 and 2 ka. The younger caldera has a diameter of ~10 km. Several small cones occur in the caldera and on the flanks. Most of the eruptive products are basalt to basaltic-andesite. A total of 12 eruptions (11 confirmed) have occurred over the last century, ranging from VEI 0 to 4. The most recent eruption (VEI 4) occurred in 2008. Zimmer et al. (2010) studied 36 olivine-, clinopyroxene-, and plagioclase-hosted melt inclusions from Okmok, and the maximum water content of 3.3 wt.% was measured in a clinopyroxene-hosted melt inclusion from sample 03OK33-1-JEB.

Okmok volcano exhibits strong deformation patterns, which has led to numerous geodetic studies and a good understanding of the plumbing system. Fournier et al. (2009) investigated GPS data collected between 2000 and 2007. In the 7 years of observation, they observed 0.5 m of uplift. Assuming a Mogi (1958) source, they determined a source depth of 3.0 km (2.5 km BSL) that is suggested to be the top of a magma storage region. Masterlark et al. (2010) performed ambient noise tomography using 40 days of data collected in 2005. They showed two low velocity anomalies exist below Okmok. The shallower anomaly (2 km deep) was suggested to be a zone of weak, fractured materials. The deeper anomaly (4-5 km, see their Fig. 7) was interpreted as a magma reservoir. This reservoir is slightly deeper than previous estimates based on geodetic data (e.g., Fournier et al., 2009), and the authors performed finite element modeling and showed that certain rheologies of the reservoir and host rock can explain the InSAR data and the depth they get. Lu and Dzurisin (2014) evaluated 20 years of InSAR data collected at Okmok. In general, they found periods of inflation led up to the eruptions in 1997 and 2008. Both periods of inflation are consistent with magma accumulation at 3.5 km depth (3.0 km BSL), which is best fit using a spherical source. They suggested that a magma reservoir exists at depths of ~2.5-4.5 km. We consider all three proposed depth ranges (3 km, 4-5 km, 2.5-4.5 km).

Seguam (Sg)

Seguam Island is located in the western extent of the Central Aleutian arc. The island is comprised of two calderas that have been built over by Holocene cones. On the eastern side is Wilcox volcano, and on the western side is Pyre Peak (1054 m). Eruptions span compositions of basalt to andesite. Two eruptions have occurred in the last 30 years, both VEI 2. The most recent eruption occurred in 1993.

Depth estimates at Seguam come from geodetic observations described by Lu and Dzurisin (2014).

Shishaldin (Sh)

Shishaldin is a prominent stratovolcano that rises to an elevation of 2857 m, making it the tallest volcano in the Aleutian Islands. Most of the edifice is constructed by basalt. Shishaldin has been very active over the last century, having 29 reported (25 confirmed) eruptions. Shishaldin commonly undergoes passive degassing. Zimmer et al. (2010) presented data on 33 olivine-hosted melt inclusions, and Rasmussen et al. (2018) evaluated 52 olivine-hosted melt inclusions. In both cases, most melt inclusions are basaltic in composition. The maximum observed water content is 2.5 wt.%, which was observed a sample of the 1999 eruption of Shishaldin (SH15DJR63, IGSN: TAP00005C).

The magmatic plumbing system of Shishaldin was studied by Cusano et al. (2015). They suggested the existence of a shallow magma reservoir at 3-5 km depth based on the occurrence of long period seismicity. Vergniolle and Caplan-Auerbach (2006) studied infrasound and seismic data from Shishaldin. We focus on the magma storage depth estimates from Cusano et al. (2015) and Vergniolle and Caplan-Auerbach (2006) here. We note that Rasmussen et al. (2018) also studied the plumbing system of Shishaldin, and they showed petrologic, seismic, and geodetic lines of evidence suggesting that magma storage is shallow (i.e., 0-3 km depth, or in the edifice). A large population of crystals contain melt inclusions that show 0-3 km entrapment depths, which were suggested to support shallow magma storage during inter-eruptive periods. Corroborating this notion is commonly observed inter-eruptive, long-period seismicity at shallow depths. During the lead up to the 1999 eruption, long period earthquakes spanned >20 km through crust, the shallowest events occurring near the long-term region of magma storage inferred from the melt inclusions. This was suggested to be a recharge event that sourced magmas from great depth (>20 km). InSAR shows a lack of eruption-related deformation, which could be, at least in part, due to storage at depths shallower than can be observed in InSAR data. Finally, a persistently active gas plume implies shallow magma storage. Taken together, these observations are robust evidence shallow storage. Rasmussen et al. (2018) questioned the longevity of this reservoir, indicating that a substantial influx of deep magma (>20 km depth) to the shallow reservoir might be required for eruption. We do not plot the depth estimates of Rasmussen et al. (2018) because they are primarily based on geochemical observations, but we note that these findings are consistent with shallow magma storage at Shishaldin, which has magmas with low water concentrations.

Tanaga (Ta)

In the Western Aleutians is Tanaga volcano, an 1806 m tall stratovolcano. The volcano consists of 2 cones, the western is the most prominent and is built within a caldera. Eruptive products range from basalt to andesite. The last known eruption was effusive and occurred in 1914. Zimmer et al. (2010) evaluated 26 olivine-, clinopyroxene-, and plagioclase-hosted melt inclusions. The highest recorded water (3.7 wt.%) was found in a basaltic pyroxene-hosted melt inclusion in sample 03TGMC-51j.

Insight into the plumbing system below Tanaga volcano comes from InSAR data investigated by Lu and Dzurisin (2014). Inflation that occurred during October-November 2005, coincident with a seismic swarm, was suggested to be related to magma intrusion. The deformation can be fit by either a Mogi (1958) source, which yields a depth of 6.5-9.5 km (5-8 km BSL), or a shallow-dipping prolate spheroid source (Yang et al., 1988), which yields a depth of 4.5-6.5 km (3-5 km BSL). Both models suggest a source that is not directly below the summit. Because both models fit the observations well, the authors suggested that a magma storage region exists between 4.5-9.5 km depth. Therefore, we consider the depth of magma storage to be 4.5-9.5 km.

Westdahl (Wd)

Westdahl volcano is a broad, voluminous volcano having a partially eroded shield-like form. The summit consists of a few peaks, including a prominent stratovolcano named Pogromni. The summit of the broader edifice is at 1563 m elevation. Most of the eruptive products are basalt to basaltic-andesite. There has been 3 confirmed eruptions in the last 100 years, which were VEI 2-3. The most recent eruption occurred in 1991-2. Rasmussen et al. (in prep) evaluated 61 olivine-hosted melt inclusions. The highest water content recorded (4.1 wt.%) was in a basaltic melt inclusion from a sample of the 1978 eruption (WD16TAP70).

Westdahl is very geodetically active, which has led to a few studies that have used InSAR and GPS to constrain the deformation source. During the 1991-2 eruption, there was a period of subsidence, which has been followed by continuous inflation through to the time of this writing. Mann and Freymueller (2003) investigated GPS data collected between 1998 and 2001. They found that during this time period, Westdahl was undergoing inflation. Assuming a point source (Mogi, 1958), they determine a source depth of $7.2^{+2.3}_{-1.2}$ km. Inflation recorded by InSAR between 1992 and 2000 can be modeled using a Mogi (1958) source, which yields a depth of 6.1-9.1 km (or 4.5-7.5 km BSL) depth (Lu and Dzurisin, 2014).

<u>Andean arc</u>

Llaima (Lm)

Llaima (3125 m) is a large, active volcano in the Southern Volcanic Zone of Chile. The cone is composed primarily of basalt to andesite, which has been built atop an 8-km-wide caldera over the last 13000 years. In the last century, there has been 30 confirmed eruptions with the vast majority being VEI 2. Bouvet de Maisonneuve et al. (2012) studied 185 olivine-hosted melt inclusions four samples of historical eruptions at Llaima. Whole rock compositions are basalt to basaltic andesite. H_2O contents of melt inclusions are variable but max out at ~4.4 wt.% (sample UF3, from an eruption in 1850).

Constraints on magma storage depth at Llaima volcano come from an InSAR study conducted by Bathke et al. (2011). They studied two periods of deformation during 2003-2008. The first phase is post-eruptive phase of deformation, which was modeled as a point source (Mogi, 1958). Deformation patterns are consistent with a source at 6-12 km. The second phase of deformation occurred as syn-eruptive inflation, and the point model indicates a source depth of 4-9 km. The authors suggest that the same reservoir is responsible for both deformational periods. We consider both 6-12 km and 4-9 km depth ranges for our work.

Cascade arc

Mount St. Helens (MSH)

Mount St. Helens is a stratovolcano (2549 m) located in Washington state in the Cascade arc, which has been built over 9 eruptive phases starting at about 40-50 ka. A prominent crater was formed during the infamous 1980 eruption, which is now the site of a dome. Eruptions have been basalt and andesite to dacite. Distinct eruptions of at least VEI 2 have occurred in 1980, 1989, 1990, and 2004.

Central American arc

Irazú (Ir)

Irazú volcano is located in the Costa Rican segment of the Central American arc. The edifice consists of a large stratocone (3432 m) with a complex of craters at the summit. Typical eruptions are explosive and consist of basalt to andesite. There have been 8 eruptions in the last century, most of which were VEI 2.

Italy

Etna (Et)

Mount Etna (3295 m) is one of the world's most active volcanoes. Much of the stratovolcano has been built by basaltic eruptions, but more alkali-rich magmas are also common. Much of the eruptive activity consists of both explosive and effusive components, which may be sourced from one of the summit vents or from a flank vent. The volcano has, more-or-less, been in a constant state of eruption over the last century, with periods of quiescence lasting no greater than a few years.

Etna is one of the most thoroughly studied volcanoes in the world. Several studies have investigated the plumbing system. Much progress has been made in studies using geodetic data (GPS, EDM, InSAR, tilt). Bonforte et al. (2008) investigate GPS data collected between 2004 and 2006, covering two eruption cycles that occurred in 2004-2005 and 2006. Contraction of sill-like source at 7.8 km depth (4.5 km BSL) occurred during the 2004-2005 eruption. Following this eruption, inflation of a vertically elongate source occurred at ~6.3 km depth (3 km BSL). Both sources are interpreted as regions of magma accumulation. The different depths may imply a

multitiered plumbing system in which different parts of the system experience periodic accumulation or withdrawal of magma. Or they might indicate that storage depth is variable. The authors summarize earlier geodetic work, which has given the following BSL depths (in km): 3.1, 3.8, 4.8, 9.3, 6.8, 4.0, 8.1, 6.2, and 2.9. Seismic. Many of the petrologic studies of magma storage at Etna have used melt inclusions as a depth control. However, none of the melt inclusions have been corrected for vapor bubble formation. So, we believe the data to be flawed and do not consider it here.

Vesuvius (Vs)

Vesusvius is an active stratovolcano (1281 m) in Italy. The cone has been built of basanites to phonolite in the caldera of Monte Somma volcano, which formed at ~17 ka. Since its inception, the volcano has hosted 8 major eruptions that have often formed pyroclastic flows. The most recent eruption occurred in 1944.

Lesser Antilles

Soufrière Hills (SH)

Soufrière Hills in an andesitic stratovolcano located in the Lesser Antilles. The summit rises to 915 m in elevation and is composed of a series of lava domes. A series of dome growth and collapse episodes has occurred over the last 20 years, with prominent eruptions in 1995, 2004, and 2005 (all VEI 3).

Four geophysical studies at Soufrière Hills Volcano help constrain the reservoir depth. Mattioli et al. (1998) look at GPS deformation patterns during 1995-1996. Using a point source model (Mogi, 1958), they find the deformation to be associated with a source at 6.5 km depth, which they associated with a magma storage region. Aspinall et al. (1998) study VT and hybrid seismicity during an eruptive phase in 1995-1997. The events they study are at depths of <7 km, which they use to suggest that magma storage occurs at ≥7 km depth. Due to the open-ended nature of this finding, we do not include the specific numbers in our depth estimate, but the findings of this study are consistent with the other results. Wadge et al. (2006) combine InSAR and GPS approaches to study deformation that occurred between 1998 and 2000. Deformation localized to the region of the lava dome is associated with conduit inflation and deflation at depths of <1 km. Deformation occurring over a broader area is associated with a deeper reservoir system, which is inflating at a depth of ~6 km BSL assuming a point source. Elsworth et al. (2008) combine geodetic and petrologic depth estimates to suggest a multi-tiered plumbing system consisting of a shallow reservoir at 6 km and a deeper reservoir at 12 km. It is possible that the preceding three studies missed the deeper reservoir and that they were all seeing the shallow reservoir of Elworth et al. (2008). However, it is also possible that they are right. So, we take 12 km from Elworth et al. (2008) combined with the other depth estimates to suggest that magma is stored between 6 and 12 km depth.

Trans-Mexican Volcanic Belt

Colima (Co)

Colima is a volcanic complex that is composed of two volcanoes: Nevado de Colima and Volcán de Colima. The latter of which reaches 3850 m in elevation and has been the location of historical eruptive activity. It has been built inside of a 5 km caldera of basaltic-andesite to andesite eruptions. There have been 16 reported (12 confirmed) eruptions in the last century, which have mostly been VEI 1. Vigouroux et al. (2008) studied 53 olivine-hosted melt inclusions in mafic samples from cinder cones near Colima. They report a maximum water content of 6.2 wt.% in a basanitic sample from Apaxtepec cone.

The seismic study of Spica et al. (2017) gives significant insight into the plumbing system below Colima. With ambient noise data, they invert for shear wave velocity and radial anisotropy. The results are used to create a 3D velocity and anisotropy models. The models give a detailed view into a multilevel reservoir system. The most distinct feature is a large (~8 km thick), elliptical magma storage region 15 km below the summit. Results of radial anisotropy analysis indicate vertical fractures spans depths of ≥35 km to the midcrustal magma reservoir, interpreted to be pathways of magma ascent from the mantle. The authors also indicate that there may exist a shallower reservoir at ~6 km depth, which is primary based on shallow seismicity (Zobin et al., 2002). We focus our attention on the larger, deeper reservoir the authors find at 15 km depth.

References

Aspinall, W., Miller, A., Lynch, L., Latchman, J., Stewart, R., White, R. and Power, J., 1998. Soufrière Hills eruption, Montserrat, 1995–1997: Volcanic earthquake locations and fault plane solutions. Geophysical Research Letters, 25(18): 3397-3400.

Bathke, H., Shirzaei, M. and Walter, T.R., 2011. Inflation and deflation at the steep-sided Llaima stratovolcano (Chile) detected by using InSAR. Geophysical Research Letters, 38(10).

Bonforte, A., Bonaccorso, A., Guglielmino, F., Palano, M. and Puglisi, G., 2008. Feeding system and magma storage beneath Mt. Etna as revealed by recent inflation/deflation cycles. Journal of Geophysical Research: Solid Earth, 113(B5).

Bouvet de Maisonneuve, C., Dungan, M.A., Bachmann, O. and Burgisser, A., 2012. Insights into shallow magma storage and crystallization at Volcán Llaima (Andean Southern Volcanic Zone, Chile). Journal of Volcanology and Geothermal Research, 211-212: 76-91.

Cusano, P., Palo, M. and West, M.E., 2015. Long-period seismicity at Shishaldin volcano (Alaska) in 2003–2004: Indications of an upward migration of the source before a minor eruption. Journal of Volcanology and Geothermal Research, 291: 14-24.

Elsworth, D., Mattioli, G., Taron, J., Voight, B. and Herd, R., 2008. Implications of Magma Transfer Between Multiple Reservoirs on Eruption Cycling. Science, 322(5899): 246-248.

Janiszewski, H.A., Abers, G.A., Shillington, D.J. and Calkins, J.A., 2013. Crustal structure along the Aleutian island arc: New insights from receiver functions constrained by active-source data. Geochemistry, Geophysics, Geosystems, 14(8): 2977-2992.

Lu, Z. and Dzurisin, D., 2014. InSAR Imaging of Aleutian Volcanoes, InSAR Imaging of Aleutian Volcanoes: Monitoring a Volcanic Arc from Space. Springer Berlin Heidelberg, Berlin, Heidelberg, pp. 87-345.

Mann, D. and Freymueller, J., 2003. Volcanic and tectonic deformation on Unimak Island in the Aleutian Arc, Alaska. Journal of Geophysical Research: Solid Earth, 108(B2).

Mann, D., Freymueller, J. and Lu, Z., 2002. Deformation associated with the 1997 eruption of Okmok volcano, Alaska. Journal of Geophysical Research: Solid Earth, 107(B4): ETG 7-1-ETG 7-12.

Mattioli, G.S., Dixon, T.H., Farina, F., Howell, E.S., Jansma, P.E. and Smith, A.L., 1998. GPS measurement of surface deformation around Soufriere Hills Volcano, Montserrat from October 1995 to July 1996. Geophysical Research Letters, 25(18): 3417-3420.

Mogi, K., 1958. Relations between the eruptions of various volcanoes and the deformation of the ground surfaces around them: Bulletin of the Earthquake Research Institute, v. 36.

Okada, Y., 1985. Surface deformation due to shear and tensile faults in a half-space. Bulletin of the seismological society of America, 75(4): 1135-1154.

Rasmussen, D.J., Plank, T.A., Roman, D.C., Power, J.A., Bodnar, R.J. and Hauri, E.H., 2018. When does eruption run-up begin? Multidisciplinary insight from the 1999 eruption of Shishaldin volcano. Earth and Planetary Science Letters, 486: 1-14.

Spica, Z., Perton, M. and Legrand, D., 2017. Anatomy of the Colima volcano magmatic system, Mexico. Earth and Planetary Science Letters, 459: 1-13.

Stelling, P., Gardner, J.E. and Begét, J., 2005. Eruptive history of Fisher caldera, Alaska, USA. Journal of Volcanology and Geothermal Research, 139(3-4): 163-183.

Syracuse, E.M., Maceira, M., Zhang, H. and Thurber, C.H., 2015. Seismicity and structure of Akutan and Makushin Volcanoes, Alaska, using joint body and surface wave tomography. Journal of Geophysical Research: Solid Earth, 120(2): 1036-1052.

Vergniolle, S. and Caplan-Auerbach, J., 2006. Basaltic thermals and Subplinian plumes: Constraints from acoustic measurements at Shishaldin volcano, Alaska. Bull Volcanol, 68(7-8): 611-630.

Vigouroux, N., Wallace, P.J. and Kent, A.J.R., 2008. Volatiles in High-K Magmas from the Western Trans-Mexican Volcanic Belt: Evidence for Fluid Fluxing and Extreme Enrichment of the Mantle Wedge by Subduction Processes. Journal of Petrology, 49(9): 1589-1618.

Wadge, G., Mattioli, G.S. and Herd, R.A., 2006. Ground deformation at Soufrière Hills Volcano, Montserrat during 1998–2000 measured by radar interferometry and GPS. Journal of Volcanology and Geothermal Research, 152(1): 157-173.

Yang, X.M., Davis, P.M. and Dieterich, J.H., 1988. Deformation from inflation of a dipping finite prolate spheroid in an elastic half-space as a model for volcanic stressing. Journal of Geophysical Research: Solid Earth, 93(B5): 4249-4257.

Zimmer, M.M., Plank, T., Hauri, E.H., Yogodzinski, G.M., Stelling, P., Larsen, J., Singer, B., Jicha, B., Mandeville, C. and Nye, C.J., 2010. The Role of Water in Generating the Calc-alkaline Trend: New Volatile Data for Aleutian Magmas and a New Tholeiitic Index. Journal of Petrology, 51(12): 2411-2444.

Zobin, V.M., Luhr, J.F., Taran, Y.A., Bretón, M., Cortés, A., De La Cruz-Reyna, S., Domínguez, T., Galindo, I., Gavilanes, J.C., Muñíz, J.J., Navarro, C., Ramírez, J.J., Reyes, G.A., Ursúa, M., Velasco, J., Alatorre, E. and Santiago, H., 2002. Overview of the 1997–2000 activity of Volcán de Colima, México. Journal of Volcanology and Geothermal Research, 117(1): 1-19.